Large Induced Interface Dipole Moments without Charge Transfer: Buckybowls on Metal Surfaces

ARTICLE *in* JOURNAL OF PHYSICAL CHEMISTRY LETTERS · NOVEMBER 2011

Impact Factor: 7.46 · DOI: 10.1021/jz2012484

THE JOURNAL OF PHYSICAL CHEMISTRY Letters

LETTER

pubs.acs.org/JPCL

Large Induced Interface Dipole Moments without Charge Transfer: Buckybowls on Metal Surfaces

Tobias Bauert,[†] Laura Zoppi,[‡] Georg Koller,[†,∥] Alberto Garcia,[§] Kim K. Baldridge,*[,‡] and Karl-Heinz Ernst*[,†,‡]

[†]Empa, Swiss Federal Laboratories for Materials Science and Technology, Laboratory for Nanoscale Materials Science, Überlandstrasse 129, 8600 Dübendorf, Switzerland

[‡]Organic Chemistry Institute, University of Zurich, Winterthurerstrasse 190, 8057 Zürich, Switzerland

[§]Institut de Ciència de Materials de Barcelona (ICMAB-CSIC), Campus UAB, 08193 Bellaterra, Spain

Supporting Information

ABSTRACT: Charge carrier injection barriers at interfaces are crucial for the performance of organic electronic devices. In this respect, tuning the electronic interface potential or, in case of the metallic electrode, the work function for electronic level alignment is crucial. However, poor control over the interface structure and the work function of the combined materials is an obstacle for better device performance. Here we show that bowl-shaped molecules, based on buckminsterfullerene, induce very large interface dipole moments of up to 8.8 D on a copper surface. It is shown experimentally and theoretically that charge transfer between both components is negligible. The origin of the large dipole moments is revealed via dispersion-enabled density functional theory, displaying a strong rearrangement of charge in the metal underneath the molecular adsorbate.

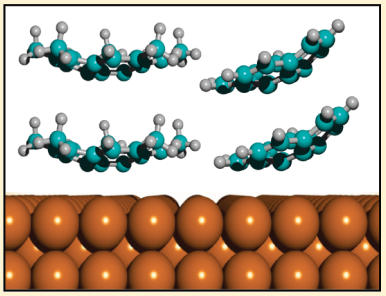

SECTION: Surfaces, Interfaces, Catalysis

The wide interest in organic semiconducting materials is driven by the wealth of their potential technological applications. At present, organic light emitting diodes (OLEDs) and simple electronic devices, such as organic field transistors (OFETs), are at the threshold of becoming commercially realized, and new applications, such as organic solar cells and chemical sensors, will follow.[1,2] One important parameter in organic device performance is the barrier of charge carrier injection, that is, the electronic level alignment between the highest occupied molecular (HOMO) and the lowest unoccupied molecular orbital (LUMO) of the organic material with respect to the Fermi level of the metallic electrode.[3] Consequently, the importance of the metal organic interface was recognized from early on,[4−6] and tailoring the work function (ϕ) for the electron transport at metal−organic interfaces was considered important.[7] On the basis of this simple band alignment picture, the following rule of thumb has been established: to minimize operational voltages, the cathode (electron injecting electrode) should be of low work function materials, while the hole injecting electrode (anode) should have a high work function. However, the work function is not a materials property per se, but depends on the interface itself, i.e., the interaction between substrate and organic adsorbate layer and therefore the resulting interface dipole.[8] As a direct consequence for tailoring organic devices, the choice for contact materials is neither guided by the work function of electrode materials nor by the intrinsic dipole of molecules. Instead of choosing low work function metals, such as magnesium, calcium, and so forth, as anode materials,[9−11] appropriate interfaces with low work functions must be designed. Another factor determining the work function is the density of surface dipoles. Naturally, only close-packed monolayer structures are useful, as open patches would simply lead to unwanted differences in the local work function and to inhomogeneous charge injection.[12] High intrinsic molecular dipoles, on the other hand, will rather cause depolarization effects without substantial influence on the work function of the electrode material. Finally, doping with alkali metals to lower the work function may even reverse the dipole moment of the hydrocarbon−electrode interface.[13]

This paper presents a combined experimental and theoretical study of the electronic properties of the Cu(111) surface modified with corannulene (**1**, $C_{20}H_{10}$, Figure 1a) and pentamethylcorannulene {**2**, $C_{20}H_5(CH_3)_5$, Figure 1c}, comparing UV-photoelectron spectroscopy (UPS) and work function change ($\Delta\phi$) measurements with dispersion-enabled density functional theory (DFT-D) calculations. The bowl-shaped polynuclear aromatic hydrocarbons, so-called buckybowls, are fragment molecules of the Buckminster fullerene buckyball C_{60} and constitute promising candidates for optoelectronic devices. We use a copper(111) electrode surface (i) to show that organic molecules can substantially lower the work function on this common electronics material, and (ii) because a single-crystal surface has the advantage that the lateral density (coverage) of the organic component is available with high accuracy. Corannulene has C_{5v}-symmetry and a π-electronic surface area comparable to that of pyrene.[14] This suggests that materials based on

Received: September 14, 2011
Accepted: October 20, 2011
Published: October 20, 2011

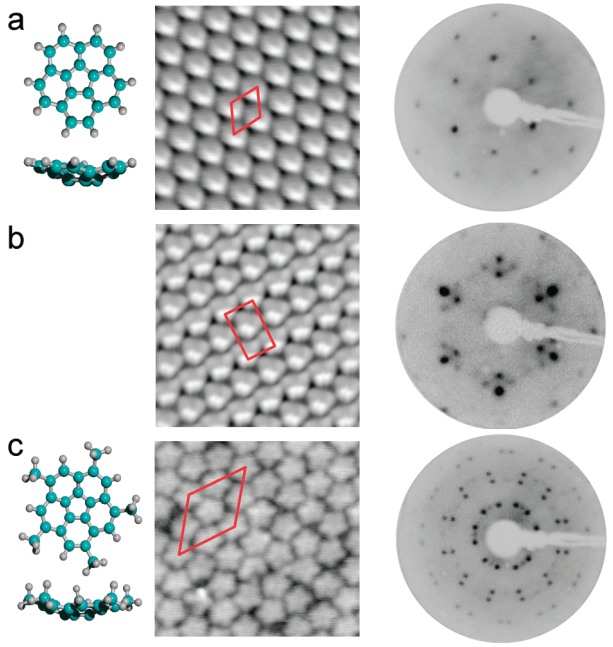

Figure 1. Ball and stick models (left) of **1** and **2**, STM images (middle, 8 nm ×8 nm) and LEED patterns (right, E_p = 14 eV) of close-packed monolayers of **1** and **2** on Cu(111). (a) (4 0, 0 4) RT polymorph of **1**, T = 253 K. (b) (4 0, 3 7) polymorph of **1**, T = 67 K. (c) (11 3, −3 8) structure of **2**, T = 56 K. The unit cells are indicated in red.

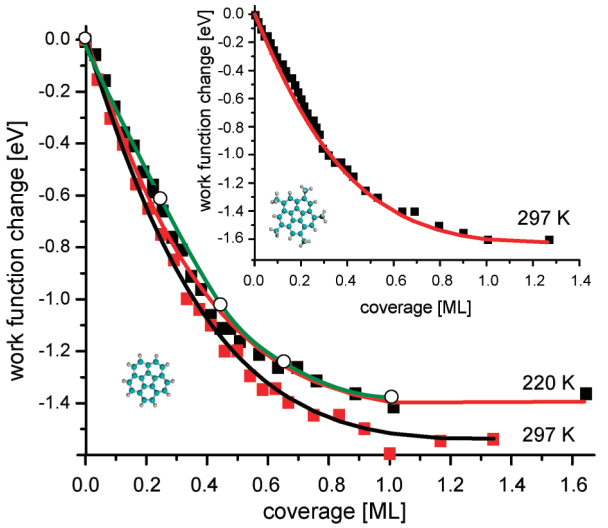

Figure 2. Work function decrease ($\Delta\phi$) versus increasing coverage for **1** and **2** (inset). The solid lines are the best-fit curves from which the dipole moment μ of the single adsorbate complex and the polarizability α were deduced via the Topping equation. The open circles represent actual calculated values via DFT-D; the green line is a fit to guide the eye.

1 should display exceptional photophysical and electrochemical properties.[15] Indeed, the intense blue-light electroluminescence, recently reported for **1**,[16] and the excellent electron acceptor ability, shown by formation of a tetraanionic species,[17,18] makes **1** and its derivatives promising candidates for applications such as OLEDs, organic photovoltaics, organic superconductors, and high energy density carbon electrodes in lithium batteries. Modification of metal surfaces with **1** and its derivatives has attracted interest previously with regard to fundamental stereochemical issues, such as symmetry-mismatch between substrate and molecules,[19,20] two-dimensional (2D) packing strategies of 5-fold-symmetric molecules,[21,22] and 2D phase transitions.[23,24]

Figure 1 shows close-packed monolayers of **1** and **2** on Cu(111). When cooling below 250 K, the monolayer of **1** undergoes a phase transition from the room temperature (RT) (4 0, 0 4) phase into a denser (4 0, 3 7) phase (Figure 1b),[23,25] followed by another phase transition at even lower temperatures into a (4 2, 0 7) phase (not shown). However, filling the contraction-induced free gaps with additional molecules at 220 K stabilizes the (4 0, 3 7) phase against the low-temperature phase transition into the (4 2, 0 7) phase.[24] In order to avoid the coexisting amorphous phase at very low temperatures,[22−24] additional molecules must be also adsorbed at 90 K until a complete (4 2, 0 7) monolayer is formed. The molecular densities are 0.90 molecule/nm^2 (≈ 1 molecule/16 Cu-atoms) for the (4 0, 0 4) phase at RT and 1.03 molecule/nm^2 (≈ 1 molecule/14 Cu-atoms) for the (4 0, 3 7) and (4 2, 0 7) phases. In all three structures, the bowl openings point away from the surface. In addition, the molecules are substantially tilted, as indicated by the nonuniform scanning tunneling microscopy (STM) appearance of the bowl rim of a single molecule.[23] This tilt has been confirmed by DFT-D, showing one of the five hexagonal carbon rings aligned parallel to the surface above a 3-fold hollow site.[23] In contrast to **1**, the dense monolayer of **2** (Figure 1c) shows no other structure than the (11 3, −3 8) RT phase upon cooling, and the STM contrast does not indicate any substantial tilt of the molecules. This is attributed to large repulsive steric interactions between one or two methyl groups at the rim and the surface in a tilted configuration. The (11 3, −3 8) phase has a density of 3 molecule/97 Cu atoms (≈ 0.60 molecule/nm^2).

UP-spectra for different coverage of **1** and **2**, representative of the electronic valence band structure of the occupied states, are presented in the Supporting Information. Briefly, the observed peaks agree well with previous gas phase spectra,[26] and they show no shift of the bands with coverage increase within the monolayer regime. Hence, the molecular orbitals are aligned to their respective local work function.[27] We note also that no change in intensity around the Fermi level is observed, which indicates that no charge transfer to the molecular LUMO occurs. From the cutoff of the secondary electrons the work function is determined. Experiment and theory delivers for the clean Cu(111) surface an absolute ϕ of 4.9 eV, in good agreement with the literature value of 4.94 eV ± 0.03 eV.[28]

The $\Delta\phi$ values for three interface-systems show a decrease with increasing coverage (Figure 2). For the completely filled monolayer the maximum $\Delta\phi$ amounts to −1.4 to −1.6 eV (Table 1). Comparing the different phases of **1**, the largest decrease in ϕ is observed for the lower density phase grown at RT. The respective interfacial dipole moments (μ) and the polarizabilities (α) for the three interfaces were extracted by applying the Topping model (Supporting Information).[29,30] Alternatively, the interface dipole moments were calculated from the initial linear decrease via the Helmholtz equation.[29,31] As a starting point for fitting the Topping model, the dipole moments obtained by the Helmholtz equation were used. It may be argued that molecules such as corannulene should be considered as extended dipoles rather then point dipoles, however, it has been shown that the results are numerically very close.[32] The solid line curves in Figure 2 represent the best fits of the Topping equation,

dx.doi.org/10.1021/jz2012484 |J. Phys. Chem. Lett. 2011, 2, 2805–2809

Table 1. Interfacial Dipole Moments and Maximum $\Delta\phi$ Values for Four Different Close-Packed Monolayers on Cu(111)

interface system on Cu(111)	dipole moment Helmholtz [Debye]	dipole moment Topping [Debye]	$\Delta\phi_{max}$ [eV]
1-(4 0, 0 4)	8.6	8.8	−1.5
1-(4 0, 3 7)	6.4	8.0	−1.4
1-(4 2, 0 7)	6.5	7.5	−1.3
2-(11 3, −3 8)	7.4	7.0	−1.6

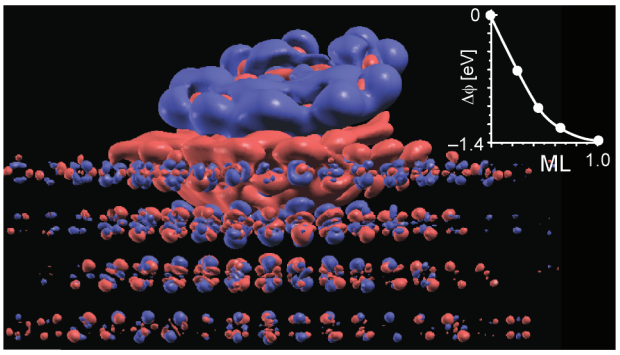

Figure 3. A strong charge cushion effect. Three-dimensional (3D) charge density difference for **1** with a C-6 ring located on top of a face-centered cubic (fcc) site of the Cu(111) surface. Red color indicates accumulation, blue color indicates depletion of charge. The isosurfaces are shown for a space charge of 0.004 e/Å^3. Only four layers of the six Cu layer slab are shown. The inset again shows the calculated work function decrease.

varying μ, α, and a correction constant for molecular mobility (n). The results for μ are listed in Table 1. Depending on the structure and method, dipole moments for the single adsorbates between 6 and 9 D are obtained. This is much larger than the 2.12 (1) and 2.35 D (2) of the free molecules. For all "Topping fits" we find $n = 0$ and $\alpha = 1.33 \times 10^{-39}$ C m^2 V^{-1} (≈ 12 Å^3). The free-molecule polarizability of **1** is 36 Å^3,[33] indicating that charge redistribution at the molecule-metal interface has occurred. The large $\Delta\phi_{max}$ values found here for the corannulene−Cu interface are in strong contrast to those reported for C_{60} on Cu(111). A (4 0, 0 4) phase is formed there as well, but with a maximum value for $\Delta\phi$ of −0.08 eV.[34] In addition, a charge transfer of 0.8 electrons per molecule from the metal into the C_{60} layer was identified by inverse photoelectron spectroscopy.[35] In general, C_{60} shows relatively small $\Delta\phi_{max}$ values on several substrates.[34]

In order to analyze the origin of the large interface dipole moment, DFT-D calculations were carried out for **1** on Cu(111) (Supporting Information), yielding an interface dipole moment of 5.8 D for the single adsorbate. Details of these calculations for this system have been published previously.[36] They reveal as the origin of the interface dipole moment a charge displacement within the whole adsorbate (Figure 3). Underneath the molecule a bowl-shaped accumulation of charge is observed, as indicated by the red cloud (blue color stands for depletion of charge). This shows that the electrons of the copper surface that usually spill-out above the surface atoms are repelled down and sideways. The physical origin for this phenomenon lies in the Pauli-exclusion-principle: the overlap of the electronic wave functions of the molecule with those of the metal is hindered, and a characteristic deformation of the metal charge is induced. This pushing back of electronic charge due to adsorption is known as the "cushion" effect.[37] Together with the push-back effect in the substrate, a depletion of charge in the molecular frame induces a substantial charge separation between the upper part of the molecule and the Cu subsurface region, leading to these tremendous interface dipole moments. The consequence is a strong electrostatic contribution to the bonding, which complements the effect of the dispersion interactions. This type of mutual-polarization binding, but at much lower strength, has been described previously, for example, for benzene on aluminum(111).[38] Despite the fact that **1** is a good electron acceptor, no charge transfer to the molecule has been observed neither in UPS (Supporting Information Figure 1) nor in the DFT calculations. This is in strong contrast to previously reported molecular large interface dipoles induced by charge transfer, as for F4-TCNQ on Cu(100), for example.[39]

In conclusion, we have shown that aromatic bowl-shaped hydrocarbons adsorbed at a metal surface can induce very large interface dipole moments without charge transfer between molecule and metal. The rearrangement of charge, in particular in the metal-molecule interface region, leads to a vertical charge separation, inducing a very large interface dipole moment. Our results offer new considerations toward interface design for electrodes in electronic devices based on organic compounds.

EXPERIMENTAL AND COMPUTATIONAL METHODS

The experiments were performed in an ultrahigh vacuum (UHV) chamber ($p < 5 \times 10^{-11}$ mbar), equipped with facilities for low energy electron diffraction (LEED), X-ray photoelectron spectroscopy (XPS), and UPS. The He I (21.2 eV) UP-spectra were recorded at 10°, 30°, and 50° electron emission angles and corresponding light incidence angles of 80°, 60°, and 40°. Work function measurements were made using the secondary electron emission cutoff measured in near normal emission with the sample biased at −9 V. Compounds **1** and **2** were synthesized as described previously.[40] The copper(111) surface (Matek, Germany) was prepared in vacuo following standard procedures.[41] The cleanliness and surface crystallinity was checked by XPS and LEED. Thermal evaporation of **1** (383 K) and **2** (413 K) was performed from effusion cells. The Cu(111) sample was cleaned by repeated cycles of Ar-ion sputtering and annealing at 800 K. Experimental LEED pattern were compared to calculated LEED patterns, generated with the LEEDpat program (K. Herrmann, FHI Berlin, M. Van Hove, City University of Hong Kong).

DFT-D, which accounts for van der Waals (vdW) interactions was used. Specifically, the RevPBE exchange-correlation potential[42] implemented in the SIESTA code[43] is supplemented with an empirical dispersion correction.[44] The Cu(111) surface has been modeled by a six-layer slab of Cu atoms where the two central layers are kept fixed at their ideal bulk positions, and two layers on each side are allowed to relax, minimizing artifacts in the calculation due to asymmetries in the free surfaces. The dimension of the supercell along the direction perpendicular to the slab is 38.1 Å. This corresponds to a vacuum space of about 25 Å in the z-direction, large enough to accommodate the adsorbed molecule without direct interaction with the periodic replicas of the slab. The Cu(111) slab geometry in the periodic surface directions is based on appropriate repetitions of the basic 1 × 1 surface unit cell, corresponding to a theoretical bulk lattice constant of 3.665 Å.

Our largest calculation involves 408 atoms, 378 of which correspond to the slab.

■ ASSOCIATED CONTENT

Supporting Information. UP valence band spectra of the different systems and from the gas phase (for **1**). UP spectra of the secondary photoelectron cutoff and the valence band for **2** with increasing coverage. Topping and Helmholtz formalism. This material is available free of charge via the Internet http://pubs.acs.org.

■ AUTHOR INFORMATION

Corresponding Authors

*E-mail: karl-heinz.ernst@empa.ch. Tel.: +41 58 765 43 63. Fax: +41 58 765 40 34. E-mail: kimb@oci.uzh.ch.

Present Addresses

[||]Present addresss: Institut für Physik, Karl-Franzens-Universität Graz, Universitätsplatz 5, 8010 Graz, Austria.

■ ACKNOWLEDGMENT

Financial support by the Swiss National Science Foundation (Project FUNDASA and 129532) is gratefully acknowledged. A. G. acknowledges support from project FIS2009-12721-C04-03 of Spain's MICINN. We thank Paul Bagus for fruitful discussions and Jay Siegel for providing the chemical compounds.

■ REFERENCES

(1) Tal, O.; Gao, W.; Chan, C. K.; Kahn, A.; Rosenwaks, Y. Measurement of Interface Potential Change and Space Charge Region Across Metal/Organic/Metal Structures Using Kelvin Probe Force Microscopy. *Appl. Phys. Lett.* **2004**, *85*, 4148–4150.

(2) Scharber, M. C.; Wuhlbacher, D.; Koppe, M.; Denk, P.; Waldauf, C.; Heeger, A. J.; Brabec, C. L. Design Rules for Donors in Bulk-Heterojunction Solar Cells — Towards 10% Energy-Conversion Efficiency. *Adv. Mater.* **2006**, *18*, 789–794.

(3) Bloom, C. J.; Elliott, C. M.; Schroeder, P. G.; France, C. B.; Parkinson, B. A. Low Work Function Reduced Metal Complexes as Cathodes in Organic Electroluminescent Devices. *J. Phys. Chem. B* **2003**, *107*, 2933–2938.

(4) Schneider, M.; Umbach, E.; Sokolowski, M. Growth-Dependent Optical Properties of 3,4,9,10-Perylenetetracarboxylicacid-dianhydride (PTCDA) Films on Ag(111). *Chem. Phys.* **2006**, *325*, 185–192.

(5) Pfeiffer, M.; Leo, K.; Zhou, X.; Huang, J. S.; Hofmann, M.; Werner, A.; Blochwitz-Nimoth, J. Doped Organic Semiconductors: Physics and Application in Light Emitting Diodes. *Org. Electron.* **2003**, *4*, 89–103.

(6) Wang, S.; Kanai, K.; Ouchi, Y.; Seki, K. Bottom Contact Ambipolar Organic Thin Film Transistor and Organic Inverter Based on C_{60}/Pentacene Heterostructure. *Org. Electron.* **2006**, *7*, 457–464.

(7) Scott, J. C. Metal—Organic Interface and Charge Injection in Organic Electronic Devices. *J. Vacuum Sci. Technol. A* **2003**, *21*, 521–531.

(8) Koller, G.; Blyth, R. I. R.; Sardar, A.; Netzer, F. P.; Ramsey, M. G. Band Alignment at the Organic—Inorganic Interface. *Appl. Phys. Lett.* **2000**, *76*, 927–929.

(9) Tang, C. W.; VanSlyke, S. A. Organic Electroluminescent Diodes. *Appl. Phys. Lett.* **1987**, *51*, 913–915.

(10) Burrows, P. E.; Forrest, S. R. Electroluminescence From Trap-Limited Current Transport in Vacuum Deposited Organic Light Emitting Devices. *Appl. Phys. Lett.* **1994**, *64*, 2285–2287.

(11) Matsumura, M.; Akai, T.; Saito, M.; Kimura, T. Height of the Energy Barrier Existing Between Cathodes and Hydroxyquinoline—Aluminum Complex of Organic Electroluminescence Devices. *J. Appl. Phys.* **1996**, *79*, 264–268.

(12) Koller, G.; Winter, B.; Oehzelt, M.; Ivanco, J.; Netzer, F. P.; Ramsey, M. G. The Electronic Band Alignment on Nanoscopically Patterned Substrates. *Org. Electronics* **2007**, *8*, 63–69.

(13) Ernst, K.-H.; Campbell, C. T. A Reversal in Dipole Moment for Adsorbed Hydrocarbons on Pt(111) Due to Coadsorbed Alkali. *Surf. Sci. Lett.* **1991**, *259*, L736–L738.

(14) Wu, Y.-T.; Siegel, J. S. Aromatic Molecular-Bowl Hydrocarbons: Synthetic Derivatives, Their Structures, and Physical Properties. *Chem. Rev.* **2006**, *106*, 4843–4867.

(15) Wu, Y.-T.; Bandera, D.; Maag, R.; Linden, A.; Baldridge, K. K.; Siegel, J. S. Multiethynyl Corannulenes: Synthesis, Structure, and Properties. *J. Am. Chem. Soc.* **2008**, *130*, 10729–10739.

(16) Valenti, G.; Bruno, C.; Rapino, S.; Fiorani, A.; Jackson, E. A.; Scott, L. T.; Paolucci, F.; Marcaccio, M. Intense and Tunable Electrochemiluminescence of Corannulene. *J. Phys. Chem. C* **2010**, *114*, 19467–19472.

(17) Ayalon, A.; Sygula, A.; Cheng, P.-C.; Rabinovitz, M.; Rabideau, P. W.; Scott, L. T. Stable High-Order Molecular Sandwiches: Hydrocarbon Polyanion Pairs with Multiple Lithium Ions Inside and Out. *Science* **1994**, *265*, 1065–1067.

(18) Aprahamian, I.; Eisenberg, D.; Hoffman, R. E.; Sternfeld, T.; Matsuo, Y.; Jackson, E. A.; Nakamura, E.; Scott, L. T.; Sheradsky, T.; Rabinovitz, M. Ball-and-Socket Stacking of Supercharged Geodesic Polyarenes: Bonding by Interstitial Lithium Ions. *J. Am. Chem. Soc.* **2005**, *127*, 9581–9587.

(19) Parschau, M.; Fasel, R.; Ernst, K.-H.; Gröning, O.; Brandenberger, L.; Schillinger, R.; Greber, T.; Seitsonen, A.; Wu, Y.-T.; Siegel, J. S. Buckybowls on Metal Surfaces: Symmetry Mismatch and Enantiomorphism of Corannulene on Cu(110). *Angew. Chem., Int. Ed.* **2007**, *46*, 8258–8261.

(20) Guillermet, O.; Niemi, E.; Nagarajan, S.; Bouju, X.; Martrou, D.; Gourdon, A.; Gauthier, S. Self-Assembly of Fivefold-Symmetric Molecules on a Threefold-Symmetric Surface. *Angew. Chem., Int. Ed.* **2009**, *48*, 1970–1973.

(21) Bauert, T.; Merz, L.; Bandera, D.; Parschau, M.; Siegel, J. S.; Ernst, K.-H. Building 2D Crystals from 5-Fold-Symmetric Molecules. *J. Am. Chem. Soc.* **2009**, *131*, 3460–3461.

(22) Merz, L.; Parschau, M.; Siegel, J. S.; Ernst, K.-H. Condensation of Fivefold-Symmetric Molecules in Two Dimensions. *Chimia* **2009**, *63*, 214–216.

(23) Merz, L.; Parschau, M.; Zoppi, L.; Baldridge, K. K.; Siegel, J. S.; Ernst, K.-H. Reversible Phase Transitions in a Buckybowl Monolayer. *Angew. Chem., Int. Ed.* **2009**, *48*, 1966–1969.

(24) Merz, L.; Bauert, T.; Parschau, M.; Koller, G.; Siegel, J. S.; Ernst, K.-H. Polymorph Selection in 2D Crystals By Phase Transition Blocking. *Chem. Commun.* **2009**, 5871–5873.

(25) Adsorbate lattices are denoted here via the (2×2) transformation matrix notation, written in $(m_{11}\ m_{12}, m_{21}\ m_{22})$ format, which links the adsorbate lattice vectors (b_1, b_2) to the substrate lattice vectors (a_1, a_2) via $b_1 = m_{11}a_1 + m_{12}a_2$ and $b_2 = m_{21}a_1 + m_{22}a_2$. See: Merz, L.; Ernst, K.-H. Unification of the Matrix Notation in Molecular Surface Science. *Surf. Sci.* **2010**, *604*, 1049–1054.

(26) Seiders, T. J.; Baldridge, K. K.; Siegel, J. S.; Gleiter, R. Ionization of Corannulene and 1,6-Dimethylcorannulene: Photoelectron Spectra, Electrochemistry, Charge Transfer Bands and *ab initio* Computations. *Tetrahedron Lett.* **2000**, *41*, 4519–4522.

(27) Kawabe, E.; Yamane, H.; Sumii, R.; Koizumi, K.; Ouchi, Y.; Seki, K.; Kanai, K. A Role of Metal d-Band in the Interfacial Electronic Structure at Organic/Metal Interface: PTCDA on Au, Ag and Cu. *Org. Electronics* **2008**, *9*, 783–789.

(28) Hölzl, J.; Schulte, F. K. In *Solid Surface Physics*; Springer Tracts in Modern Physics; Hohler, G., Ed.; Springer: Berlin, Germany, 1979; Vol. 85.

(29) Fukagawa, H.; Yamane, H.; Kera, S.; Okudaira, K. K.; Ueno, N. Experimental Estimation of the Electric Dipole Moment and Polarizability of Titanyl Phthalocyanine Using Ultraviolet Photoelectron Spectroscopy. *Phys. Rev. B* **2006**, *73*, 041302/1–4.

(30) Verhoef, R. W.; Asscher, M. The Work Function of Adsorbed Alkalis on Metals Revisited: A Coverage-Dependent Polarizability Approach. *Surf. Sci.* **1997**, *391*, 11–18.
(31) Ernst, K.-H.; Christmann, K. The Interaction of Glycine with a Platinum (111) Surface. *Surf. Sci.* **1989**, *224*, 277–310.
(32) Maschhoff, B. L.; Cowin, J. P. Corrected Electrostatic Model for Dipoles Adsorbed on a Metal Surface. *J. Chem. Phys.* **1994**, *101*, 8138–8151.
(33) Malloci, G.; Joblin, C.; Mulas, G. On-Line Database of the Spectral Properties of Polycyclic Aromatic Hydrocarbons. *Chem. Phys.* **2007**, *332*, 353–359 (http://astrochemistry.ca.astro.it/database/).
(34) Tsuei, K.-D.; Yuh, J.-Y.; Tzeng, C.-T.; Chu, R.-Y.; Chung, S.-C.; Tsang, K.-L. Photoemission and Photoabsorption Study of C_{60} Adsorption on Cu(111) surfaces. *Phys. Rev. B* **1997**, *56*, 15412–15420.
(35) Tsuei, K.-D.; Johnson, P. D. Charge Transfer and a New Image State of C_{60} on Cu(111) Surface Studied by Inverse Photoemission. *Solid State Commun.* **1997**, *101*, 337–341.
(36) Zoppi, L.; Garcia, A.; Baldridge, K. K. Theoretical Investigation of the Binding Process of Corannulene on a Cu(111) Surface. *J. Phys. Chem. A* **2010**, *114*, 8864–8872.
(37) Witte, G.; Lukas, S.; Bagus, P. S.; Wöll, C. Vacuum Level Alignment at Organic/Metal Junctions: "Cushion" Effect and the Interface Dipole. *Appl. Phys. Lett.* **2005**, *87*, 263502/1–3.
(38) Duschek, R.; Mittendorfer, F.; Blyth, R. I. R.; Netzer, F. P.; Hafner, J.; Ramsey, M. G. The Adsorption of Aromatics on sp-Metals: Benzene on Al(111). *Chem. Phys. Lett.* **2000**, *318*, 43–48.
(39) Katayama, T.; Mukai, K.; Yoshimoto, S.; Yoshinobu, J. Thermally Activated Transformation from a Charge-Transfer State to a Rehybridized State of Tetrafluoro-tetracyanoquinodimethane on Cu(100) *J. Phys. Chem. Lett.* **2010**, *1*, 2917–2921.
(40) Seiders, T. J.; Elliott, E. L.; Grube, G. H.; Siegel, J. S. Synthesis of Corannulene and Alkyl Derivatives of Corannulene. *J. Am. Chem. Soc.* **1999**, *121*, 7804–7813.
(41) Ernst, K.-H.; Kuster, Y.; Fasel, R.; Müller, M.; Ellerbeck, U. Two-Dimensional Separation of [7]Helicene Enantiomers on Cu(111). *Chirality* **2001**, *13*, 675–678.
(42) Zhang, Y.; Yang, W. Comment on "Generalized Gradient Approximation Made Simple. *Phys. Rev. Lett.* **1998**, *80*, 890–890.
(43) Soler, J. M.; Artacho, E.; Gale, J. D.; Garcia, A.; Junquera, J.; Ordejon, P.; Sanchez-Portal, D. The SIESTA Method for *ab initio* Order-N Materials Simulation. *J. Phys. C: Condens. Matter* **2002**, *14*, 2745–2779.
(44) Grimme, S. Semiempirical GGA-Type Density Functional Constructed with a Long-Range Dispersion Correction. *J. Comput. Chem.* **2006**, *27*, 1787–1799.